JOURNAL OF MATERIALS SCIENCE 20 (1985) 1660–1670

EPR study of the influence of defect structure on electrical properties of ZnO varistors

M. V. VLASOVA, N. G. KAKAZEY
The Institute for Development of Materials AS USSR, Kiev, USSR
P. KOSTIĆ, O. MILOŠEVIĆ, D. USKOKOVIĆ
The Institute of Technical Sciences of the SASA, Beograd, Yugoslavia

The influence of the defect structure of ZnO grains on the electrical properties of ZnO varistors, on sintering parameters and temperature of subsequent heat treatment, was studied. By analysis of the Mn^{2+} spectrum obtained by the electron paramagnetic resonance technique, the dependence of electrical properties of ZnO varistors on the defect structure of ZnO grains and impurity ions, was shown.

1. Introduction

The potential barrier, formed at the point of contact of two ZnO grains, is of vital importance for non-ohmic properties of multiphase ZnO ceramics. The greatest influence on the potential barrier and, consequently, on the attainment of high non-linearity is caused by manganese, and also bismuth [1]. The distribution of donor atoms of manganese and bismuth inside ceramics is essential. Manganese atoms and eventually cobalt and aluminium atoms have to be located in ZnO grains [2], but impurities, in particular bismuth, need not diffuse into the surface layer of grains, but only to be present along grain boundaries, to disturb the crystal structure of zinc oxide. Manganese inclusions in ZnO grains form intersection points of zinc- and oxygen-vacancy concentrations, resulting in the potential barrier [3]. The defect structure of ZnO grains and the presence of impurities in the grain surface layer have not yet been studied by electronic paramagnetic resonance (EPR). The aim of this paper was to contribute to a better understanding of the mechanism of potential barrier formation and the changes in the electrical properties of ZnO varistors using the EPR technique.

2. Theory

The existence of a spectrum, which may be attributed to Mn^{2+} ions, was noticed when using the EPR method (Fig. 1). It is located in the crystal field of axial symmetry. Observation of the response signal of fine structure lines made easier the identification of the spectrum, which may be described by the spin Hamiltonian:

$$\mathcal{H} = g\beta HS + D[S_z^2 - \tfrac{1}{3}S(S+1)] + ASI, \quad (1)$$

where g is the factor of spectroscopic splitting, β the Bohr magneton, S the effective-spin operator, A the constant of the isotropic ultra-fine effect, H the intensity of the magnetic field, D the axial distortion parameter, and I the absorption intensity.

The general relationship between resonant transitions in the magnetic field and the crystal orientation is known, which accounts for the corrections for higher orders [4, 5]. We shall use this relationship to find the position of the response signal in polycrystalline samples. By the standard method it is easy to show that the response signals of fine structure lines appear in the positions corresponding to the crystal orientation of $\theta_1 = 90^\circ$ for all fine structure lines, and $\theta_2 \sim 57^\circ$ for the transition $-1/2, m \leftrightarrow 1/2, m$ only. Therefore, the position of the response signal is given by the expressions:

for transition $-1/2, m \leftrightarrow 1/2, m$:

0022-2461/85 $03.00 + .12 © *1985 Chapman and Hall Ltd.*

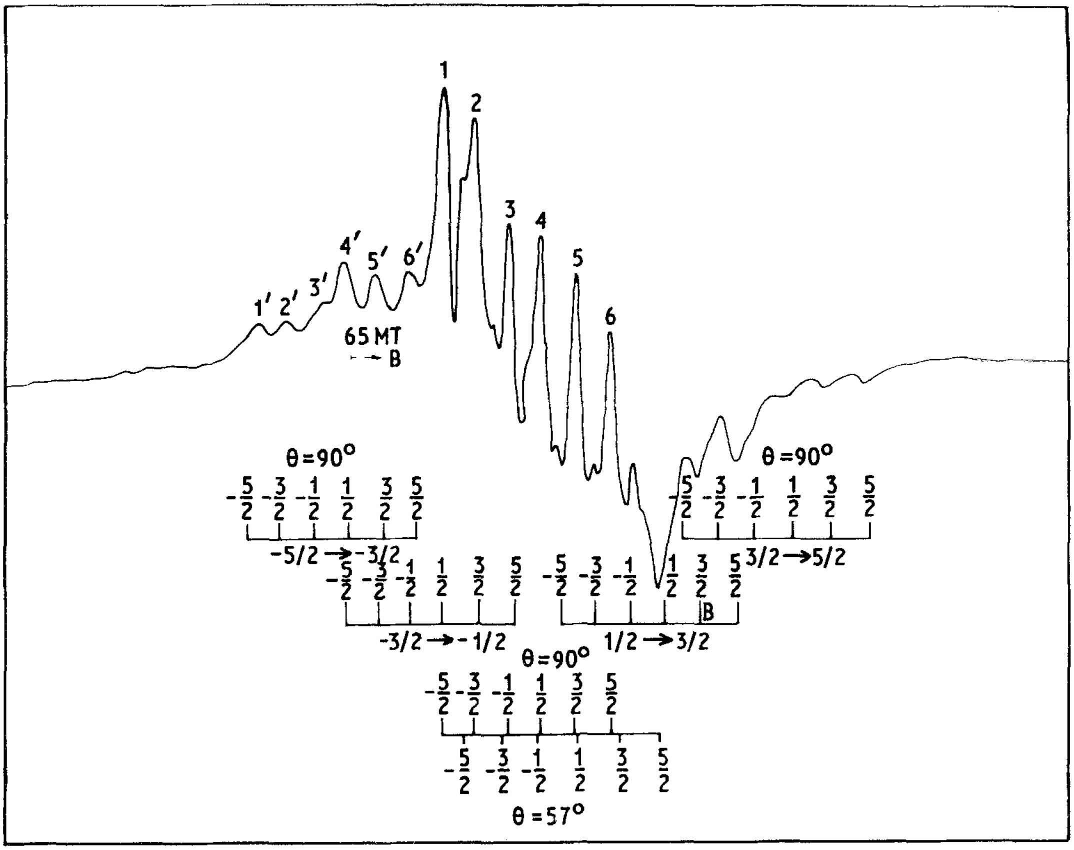

Figure 1 Typical shape of the EPR spectrum of Mn^{2+} ions in multiphase ZnO ceramics. Calculation of the response signal position is illustrated below the spectrum.

$$H_{\theta_1} = H_0 - \frac{2D^2}{H_0} - Am - \frac{A^2}{2H_0}(\tfrac{35}{4} - m^2) + \frac{2D^2Am}{H_0^2} \qquad (2)$$

$$H_{\theta_2} = H_0 + \frac{2.2D^2}{H_0} - Am - \frac{A^2}{2H_0}(\tfrac{35}{4} - m^2) - \frac{28D^2Am}{H_0^2}; \qquad (3)$$

for transition ± $1/2, m \leftrightarrow \pm 3/2, m$:

$$H'_{\theta_1} = H_0 \pm D \mp \frac{5D^2}{4H_0} - Am - \frac{A^2}{2H_0}(\tfrac{35}{4} - m^2 + 2m) \pm \frac{5D^2Am}{4H_0^2}; \qquad (4)$$

for transition ± $3/2, m \leftrightarrow \pm 5/2, m$:

$$H''_{\theta_1} = H_0 \mp 2D \mp \frac{D^2}{H_0} - Am - \frac{A^2}{2H_0}(\tfrac{35}{4} - m^2 + 4m) \pm \frac{D^2Am}{H_0^2}. \qquad (5)$$

Estimating the response signal position in the magnetic field (as the standard g-factor we used only MgO with Cr^{3+} and Mn^{2+} additives) it is easy to find the spin Hamiltonian parameters by means of previous equations:

$$g = 2.001 \pm 0.0005; \quad D = 25 \pm 0.2\,\text{MT};$$
$$A = 7.92 \pm 0.04\,\text{MT}.$$

These data are in good agreement with those already published for Mn^{2+} ions in ZnO crystals [6]. They were used as a basis for the following analysis.

The superposition of different lines of the fine structure and the impossibility of following exactly the change in amplitude, width and shape of separate spectrum components and their mechanisms of deformation, make the problem of obtaining useful information from the spectra obtained at first sight unsolvable. However, we will not introduce a large error if we accept that the amplitude and shape of the response signal in polycrystals are determined to the greatest extent by the width and shape of a given transition in the orientation of the response signal appearance. In addition, the amplitudes of separate transition lines, in the range of one superfine group, are significantly different, because of the various conditions of finding average values as well as in the different widths of individual lines ($\Delta H_{3/2 \leftrightarrow 5/2} > \Delta H_{1/2 \leftrightarrow 3/2} > \Delta H_{-1/2 \leftrightarrow 1/2}$). Hence in the case of the response signal emanating from the transition $1/2 \leftrightarrow 3/2$ to the transition signal $3/2 \leftrightarrow 5/2$, the resulting signal amplitude results mainly from the amplitude of the first signal. In this work the response signals of the transitions $-1/2 \leftrightarrow 1/2$ (orientation 90°) (Fig. 1, nos. 1 to 6) and $\pm 1/2 \leftrightarrow \pm 3/2$ (orientation 90°, Sign 1′–6′ on Fig. 1) were measured. This enabled a rather correct estimation of the general character of the signal amplitude change of its dependence on treatment conditions. However, there is a series of causes of the change in individual line widths and hence also of response signal amplitude:

1. the dipole–dipole broadening is caused by the change in paramagnetic impurity concentration;
2. relaxation broadening occurs as a result of the change in relaxation time of transition;
3. deformation broadening occurs as a consequence of crystal lattice deformation.

We shall briefly consider which changes in signals 3 and 4′ may appear because of the different broadening mechanisms. At pure dipole–dipole interaction of the same ions, the mean line width is [7]:

$$n^2\langle(\Delta\nu)^2\rangle = 3S^+(S^+ + 1) \times \sum_j \frac{g^4\beta^4}{r_{ij}} f\left(\frac{1 - 3\cos^2\theta_{ij}}{2}\right)^2 . \qquad (6)$$

The summation term is common for all transitions and hence transition is determined by the spin volume. Therefore, the ratio of the amplitude of different transitions is independent of impurity concentration. In the case of relaxation broadening, i.e. the change in relaxation time of each transition, there is the same dependence on spin (for example on account of the change in sample temperature). Crystal lattice deformation may occur as a consequence of the existence of different point and line defects. The type of deformation may be different, but we may assume that their existence brings about the scattering of parameters of the axial field, D. According to Stonehem [8] the presence of lattice defects causes signal movement as well as broadening. Using Equations 2 to 5 for the calculation of movement of the response signal on account of the change $D_0 \rightarrow D_0 + \Delta D$ we obtain:

$$\Delta H_{-1/2\rightarrow 1/2} = H_{D_0} - H_{D_0+\Delta D} = \frac{4D\Delta D}{H_0} + \frac{4D\Delta D A m}{H_0^2} \qquad (7)$$

$$\Delta H_{\pm 1/2\rightarrow \pm 3/2} = H_{D_0} - H_{D_0+\Delta D} = \mp D \mp \frac{5D\Delta D}{2H_0} \pm \frac{2D\Delta D A m}{H_0^2} \qquad (8)$$

$$\Delta H_{\pm 3/2\rightarrow \pm 5/2} = H_{D_0} - H_{D_0+\Delta D} = \mp 2\Delta D \mp \frac{2D\Delta D}{H_0} \pm \frac{2D\Delta D A m}{H_0^2} . \qquad (9)$$

From these equations it follows that non-central transitions, at the existence of defects, broaden much more than the central one. Hence, the ratio of response signal amplitudes, J_3/J'_4, may be used as a qualitative measure of some internal changes inside the ZnO lattice. For example, an increase in this ratio is proof of a deformation phenomenon in the samples.

3. Experiments

Four systems, each containing ZnO with additives of Bi_2O_3, MnO_2, CoO and Sb_2O_3, were prepared by conventional ceramic methods and sintered in the temperature range 1373 to 1673 K. System 1 contained SnO_2 and Al_2O_3 as well as the oxides mentioned. System 2 was obtained by the addition of K_2O. System 3 contained Cr_2O_3 instead of SnO_2 and system 4 was prepared when Al_2O_3 was added to the basic composition. Systems 3 and 4 were subsequently treated to enable the reaction between the total quantity of additives and a part of the total content of ZnO to occur. From all the electrical characteristics the coefficient of non-linearity was chosen to be determined. It was estimated from the curve of applied electric field current density over the range 10 to 100 A m^{-2}. A typical curve in the case of the systems 3 and 4 is shown in Fig. 2.

4. Results and discussion

4.1. Conditions of calcination

The role of calcination is to reduce the level of imperfection of the ZnO lattice. Calcination at 973 K does not result in a total recovery of the

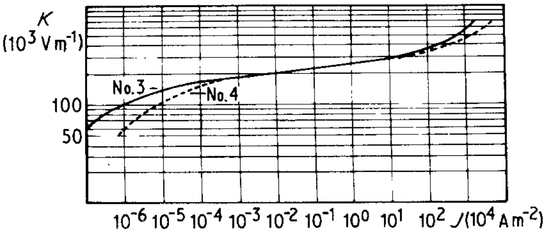

Figure 2 Current–voltage characteristics of the systems 3 and 4.

initial defect structure. Hence, sintering of these samples at 1473 K enhances diffusion of Mn^{2+} and other ions (Co^{2+}, Sb^{3+}, Bi^{3+}, Al^{3+}, Sn^{4+}), which are able to deform the area around the Mn^{2+} ions in the ZnO lattice. This is confirmed by higher values of the ratio J_3/J_4' (Fig. 3a). It appears that the defect structure of initial particles recovers more by calcination at 1073 K (and also at 1173 K). In the non-deformed ZnO lattice, only Mn^{2+} and Co^{2+} ions are able to diffuse. This means that deformations in the case of ZnO powder calcinated at 973 K, appear because of the multivalent ions, in addition to Mn^{2+}, introduced into the ZnO lattice. This process brings about the destruction of an inverse surface layer of ZnO grains, which is responsible for the formation of the potential barrier [3]. Because of this, non-linear characteristics are lost and the value of the non-linearity coefficient is reduced (Fig. 3b).

4.2. Sintering temperature

An increase in lattice deformation degree (J_3/J_4') with increasing sintering temperature, in the case of the system 1, calcinated at 973 K (Fig. 4a), is caused by the intensification of diffusion (on account of remaining defects) of multivalent impurities inside the ZnO lattice. Attainment of a maximum and structure ordering may be the consequence of the following processes:

1. the enhanced recovery of initial defects, because multivalent impurities may diffuse only into a thin surface layer;
2. the rate of increase of the evaporation of a component which participates most actively in the deformation of surrounding Mn^{2+}. On the basis of a series of data [9–11], it is thought that this component may be bismuth oxide.

In the case of samples containing ZnO powder calcinated at 1173 K, a significant insertion of multivalent impurities into the ZnO lattice occurs only at 1473 K (Fig. 4b). The extreme value of non-linearity coefficients corresponds to an extreme value of the ratio J_3/J_4' (Figs. 5a and b). This means that the decrease in the potential barrier is caused by the partial neutralization of the p-ZnO surface layer (by the insertion of impurities as well as by the evaporation of bismuth oxide).

The previous system was dopped with 0.5 mol % K_2O and sintered under identical conditions.

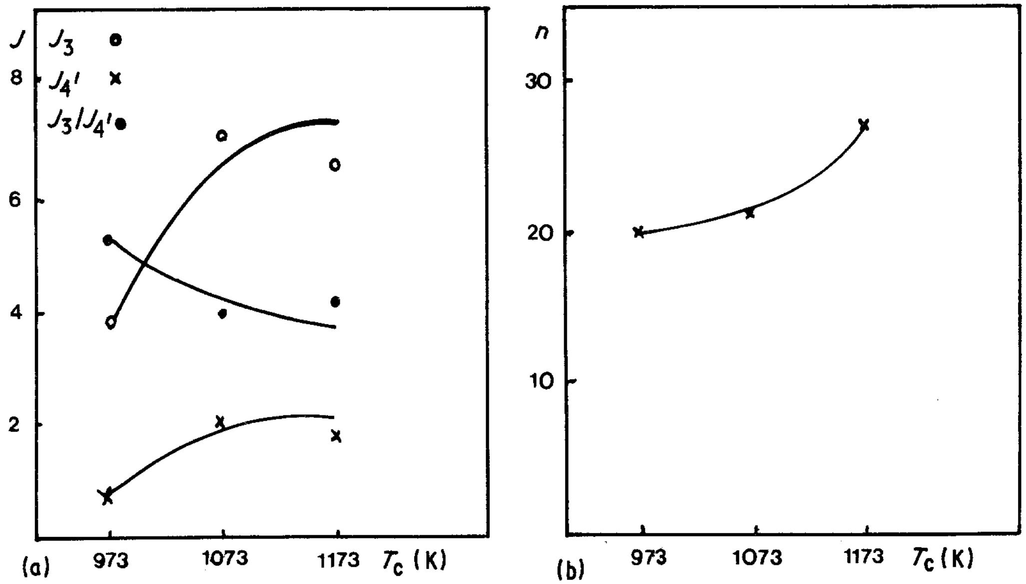

Figure 3 (a) Response signal amplitude as a function of calcination temperature (system 1). (b) The non-linearity coefficient as a function of calcination temperature (system 1).

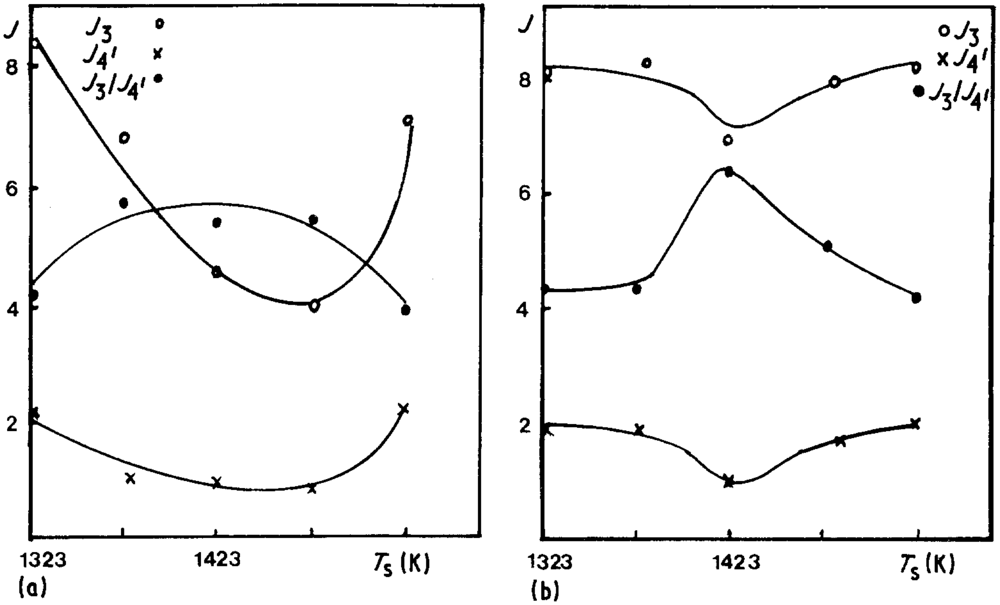

Figure 4 Response signal amplitude as a function of sintering temperature for system 1:(a) $T_c = 973$ K; (b) $T_c = 1173$ K.

The results obtained (Fig. 6a) may be analysed for the attenuation of total signal intensity (for example on account of the reduction of inserted impurities) with no changes in the defect state, as well as for dipole–dipole broadening. The equalization of superfine component amplitudes of central transitions indicates the dipole–dipole mechanism of registered spetral broadening. The observed changes are possible in the case of an approximately constant concentration of Mn^{2+} ions in ZnO. However, their localization in the area of a particle changes from in the bulk, for samples sintered at lower temperatures, to at the surface for samples sintered at higher temperatures. Since K_2O is a relatively low-melting oxide, its role is reduced to ZnO grain-coating, i.e. the inhibition of volume alloying of ZnO with Mn^{2+} ions. The absence of an abrupt rise of imperfection

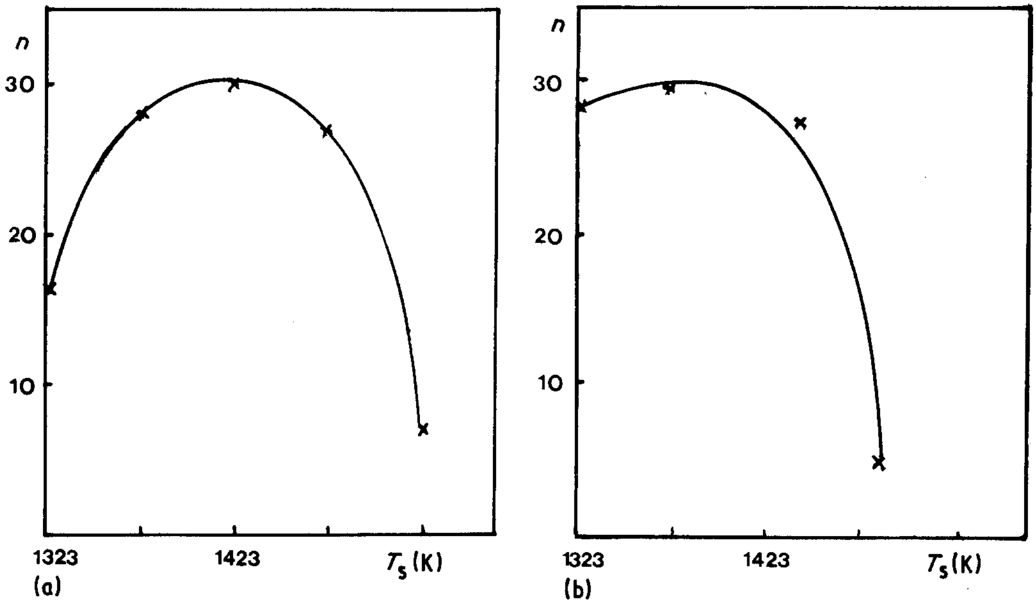

Figure 5 The non-linearity coefficient as a function of sintering temperature; (a) $T_c = 973$ K; (b) $T_c = 1173$ K.

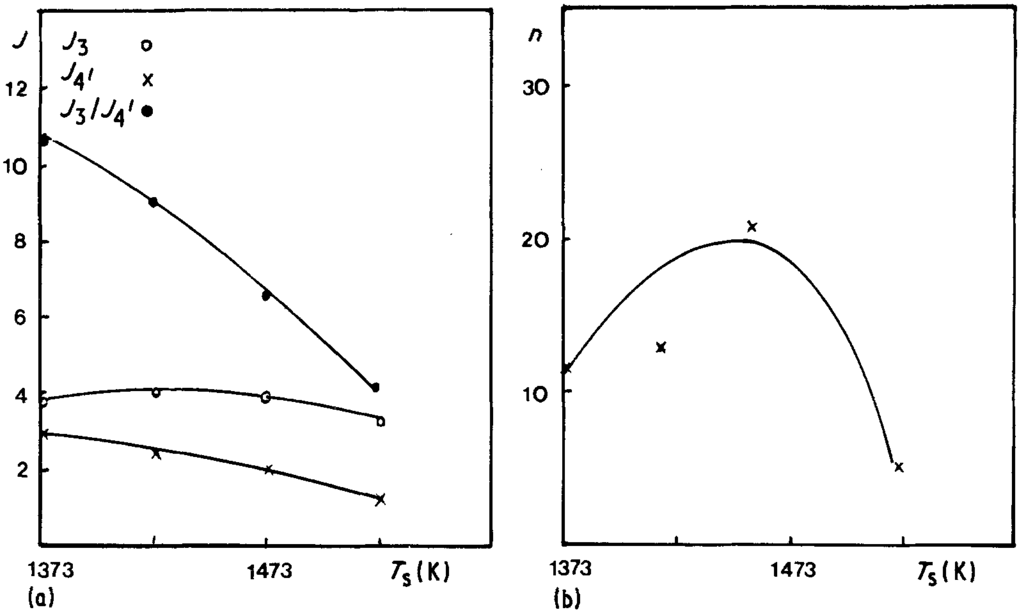

Figure 6 (a) The response signal amplitude and (b) the non-linearity coefficient as functions of sintering temperature for system 2.

at 1473 K, observed in the case of samples without K_2O, also indicates the inhibiting role of K_2O in the process of bismuth ion insertion into ZnO grains. Since it also inhibited the diffusion of Mn^{2+} ions, which is important for the potential barrier formation, the influence of K_2O on the varistor non-linearity is negative (Fig. 6b).

In the case of the system in which the mixture of additives and a portion of ZnO have been previously treated, and which does not contain Al_2O_3, the analysis of the EPR spectra indicated that, in addition to the already mentioned spectrum of Mn^{2+} in ZnO, there is another asymmetrical signal with $g = 4.3$. Usually such signals are caused by the existance of ions in s-states (Mn^{2+}, Cr^{3+}) distributed in an intensively deformed crystal field. This enabled us to attribute the spectrum to Mn^{2+} ions, which are present in the lattice of one of the complex compounds formed. The appearance of the signal in the case of the pyrochlore phase synthesized in advance makes this assumption reasonable. Fig. 7a shows the change of EPR signal amplitude with sintering temperature. It should be noted that the signal intensity of Mn^{2+} in ZnO is about half that in the case analysed previously. It is probably a consequence of the various methods of mixture preparation. The increase in sintering temperature has practically no influence on the quantity of Mn^{2+} in ZnO, although there is a small increase in the imperfection degree of the ZnO phase at sintering temperatures higher than 1523 K. This temperature is also characteristic, because a maximum signal was observed at $g = 4.3$. The increase in the amplitude of this signal (up to 1523 K) is caused by the enlargement of the pyrochlore phase content, owing to the subsequent reaction. The following reduction of intensity is a consequence of the decomposition of the pyrochlore phase in to the spinel and Bi_2O_3 [12]: The non-linearity coefficient of this system (Fig. 7b) retains a high value up to 1653 K, but above this temperature an abrupt drop in non-linearity occurs. This is in accordance with the maximum value of J_3/J_4' (at ~ 1653 K). The surface layer of ZnO is extremely sensitive to the presence of ions (specially heavier ions). Decomposition of the pyrochlore phase in to the spinel and Bi_2O_3 (a decrease in the signal $J_{g=4.3}$) causes an increase in the number of free bismuth ions, which may diffuse into the grain surface layer neutralizing the area of space charge, and in this way the potential barrier as well. This is possible owing to the rather high sintering temperatures. Since a temperature rise brings about the evaporation of bismuth, which is the second important factor in the formation of the potential barrier, the non-linearity coefficient retains its low values. It

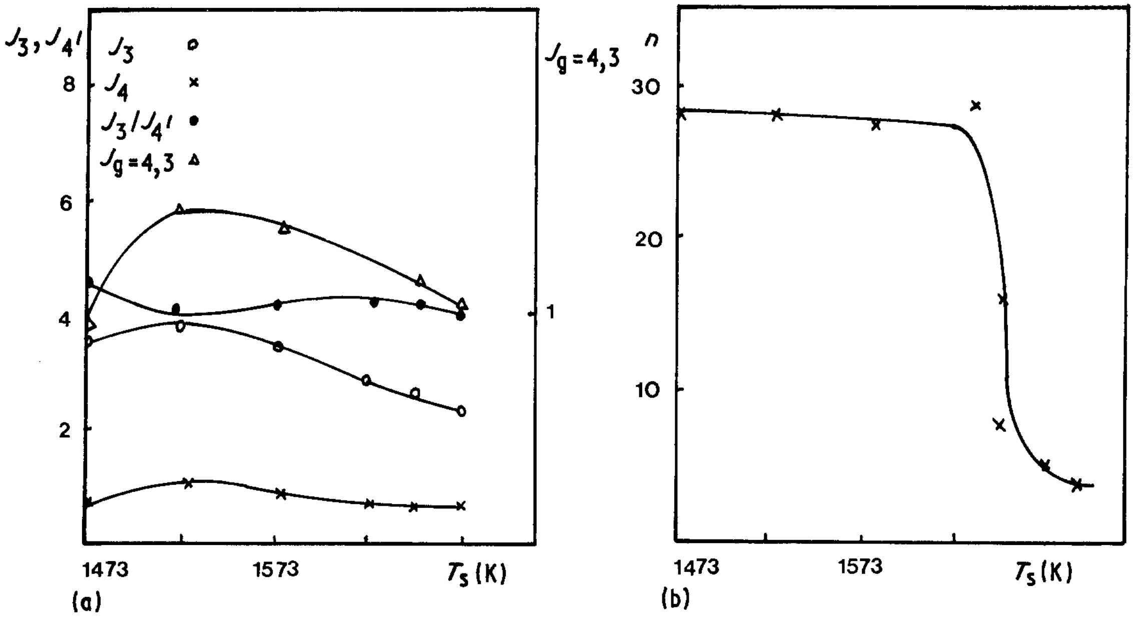

Figure 7 (a) The response signal amplitude and (b) the coefficient of non-linearity as functions of sintering temperature (system 3).

corresponds again to the decrease in the signal intensity, J_3/J_4', and to a further reduction and decomposition of the pyrochlore phase.

4.3. Sintering time

A gradual increase of the quotient J_3/J_4' with prolonged sintering time, in systems 1 and 2, reflects the kinetics of insertion of impurities which deform the areas around Mn^{2+} ions (Figs. 8a and b). If sintering temperature is higher, a shorter time will be needed for the insertion of the same quantity of impurities that deform the lattice. The evaporation of bismuth oxide during prolonged sintering, once more emphasizes the role of Bi_2O_3 in the broadening of Mn^{2+} signals in samples sintered for short time intervals. The extreme shape of the signal J_3 is conditioned by two competitive processes: the increase in J_3 is the

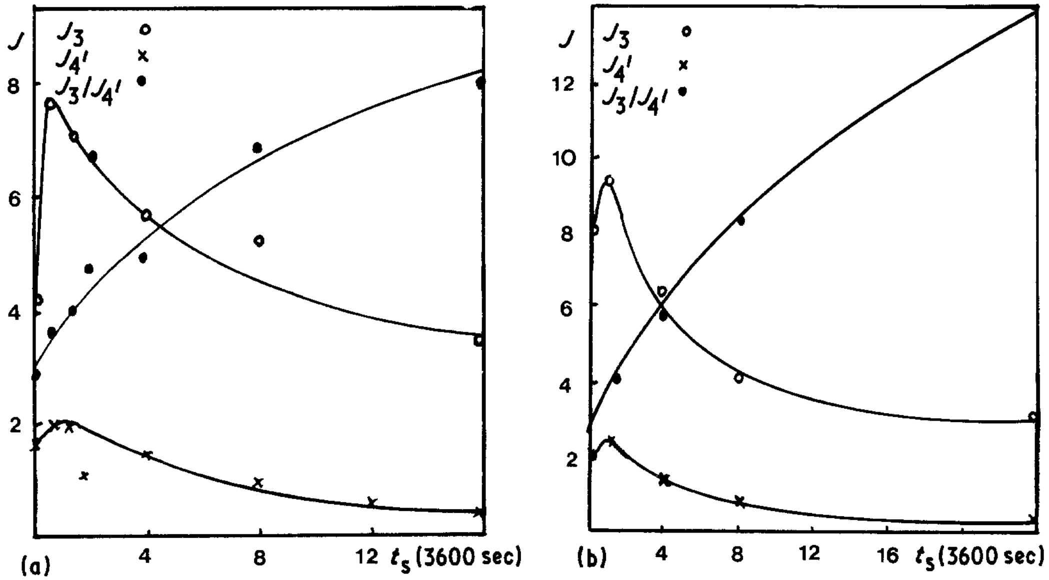

Figure 8 The response signal amplitude as a function of sintering time ($T_s = 1423$ K); (a) system 1; (b) system 2.

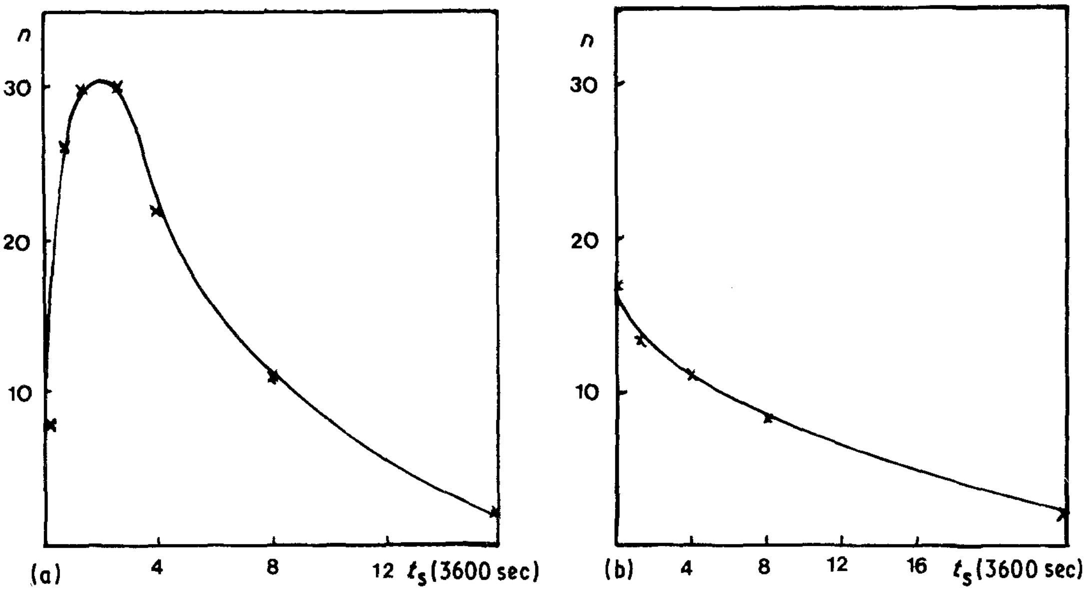

Figure 9 The non-linearity coefficient vs sintering time (T_s = 1423 K). (a) System 1, (b) System 2.

relationship with a greater content of impurities in ZnO; the decrease in J_3 corresponds to deformation broadening. The dependence of non-linearity on sintering time (Figs. 9a and b) justifies the assumption about the relationship between the decrease in potential barrier height and the insertion of a definite characteristic quantity of impurities into a thin surface layer of ZnO grains.

During prolonged sintering the added K_2O also activates insertion of other impurities which deform the areas around the Mn^{2+} ions (Fig. 8b). However, since K_2O inhibits the volume alloying of ZnO grains with manganese ions, the non-linearity coefficient decreases monotonically in the range studied, because manganese concentration in ZnO grains cannot reach the value required for a high non-linearity coefficient. At the same time, bismuth participates in the destruction of the potential barrier.

The influence of the sintering time, in the case of samples with a predicted mixture of additives with a portion of ZnO (system 4), is reflected mainly in the increase of amplitude of the signal with $g = 4.3$, i.e. of the pyrochlore phase (T_s = 1473 K) (Fig. 10a). At the same time, less ZnO defect lattice is formed, owing to lower stresses, which are important during the existence of partially reacted components forming the pyrochlore phase. Fig. 10b illustrates that bismuth oxide, obtained from the pyrochlore phase, causes a reduction in the non-linearity coefficient, disturbing the p-layer of ZnO grains.

4.4. Cooling rate

Samples of system 1 were rapidly cooled causing thermal stresses inside the material (Fig. 11a). This leads to the maximum deformation areas around Mn^{2+} in the ZnO grains. A lower cooling rates enables one to obtain samples with lower stresses.

The increase of deformations inside slower cooled samples is most probably caused by a partial insertion of other impurities into the ZnO lattice. However, the value of the non-linearity coefficient is not conditioned solely by thermal stresses formed inside the samples, but also by the impossibility of forming an intersection point between the concentration of zinc-vacancies and oxygen-vacancies in the surface layer of ZnO grains [2, 3], and in such a way a corresponding potential barrier as well. All this occurs because the diffusion of defects to the grain surface was made impossible. The non-linearity reduction caused by the decrease of cooling rate coincides with the observed insertion of impurity ions in a thin surface layer of ZnO grains. The space charge is neutralized and thus the potential barrier is reduced to a value determined by the "disordered layer", formed by bismuth ions on the grain surface (Fig. 11b). The optimal value of cooling rate is 1.5 to 5° C min^{-1}.

4.5. Subsequent thermal treatment

Samples containing a mixture of additives with Al_2O_3, were sintered at 1473 K for 4 h and then

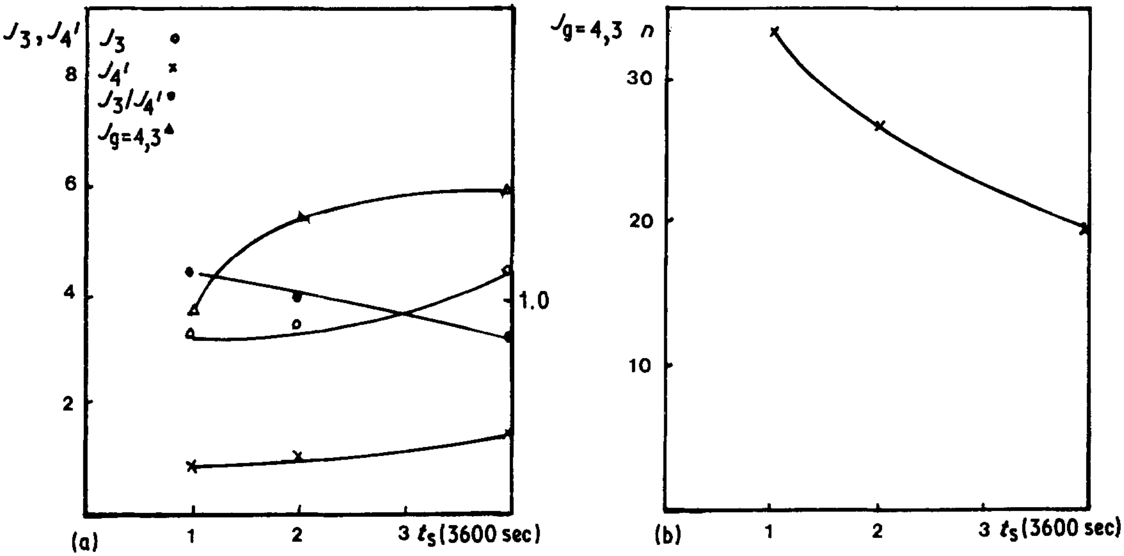

Figure 10 (a) The response signal amplitude and (b) the non-linearity coefficient as functions of sintering time (system 4, $T_s = 1473$ K).

thermally treated for 1 h. At 673 K the maximum amplitude of the Mn^{2+} signal in ZnO and the pyrochlore phase ($g = 4.3$) was observed, and at the same time the deformation degree of the ZnO crystal structure (J_3/J_4') was minimal (Fig. 12a). Since at 673 K there is a small probability for ion insertion into the ZnO lattice, the observed changes are obviously conditioned by the recovery of the retained thermal stresses (up to 673 K) as well as by the formation of such a stress on account of the partial reconstruction of the pyrochlore phase (over 673 K). It is interesting to note that in the case of samples thermally treated at 1073 K, a new signal with $g \approx 3$ was observed. However, we do not aim to discuss its origin at present. The maximum value of the non-linearity coefficient was obtained at ~ 673 K (Fig. 12b), coinciding with the maximum values of the signals J_3, J_4 and $J_{g=4.3}$ and with the minimum values of J_3/J_4'. This may be explained by a decrease in the impurity ion concentration inside the ZnO grains and, consequently, inside the surface layer

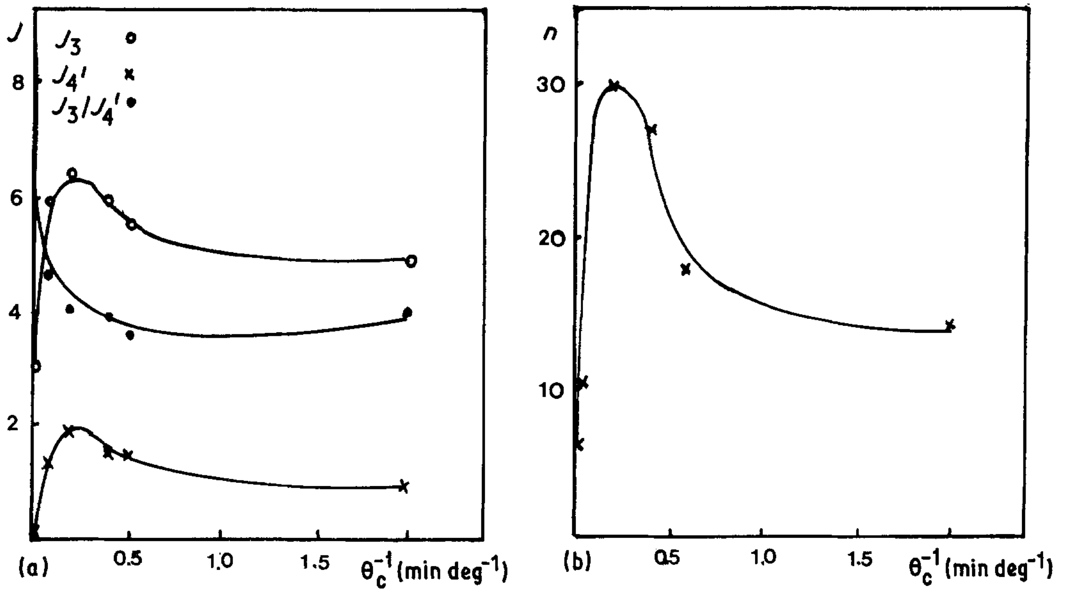

Figure 11 (a) The response signal amplitude and (b) the non-linearity coefficient at functions of cooling rate (system 1, $T_s = 1423$ K).

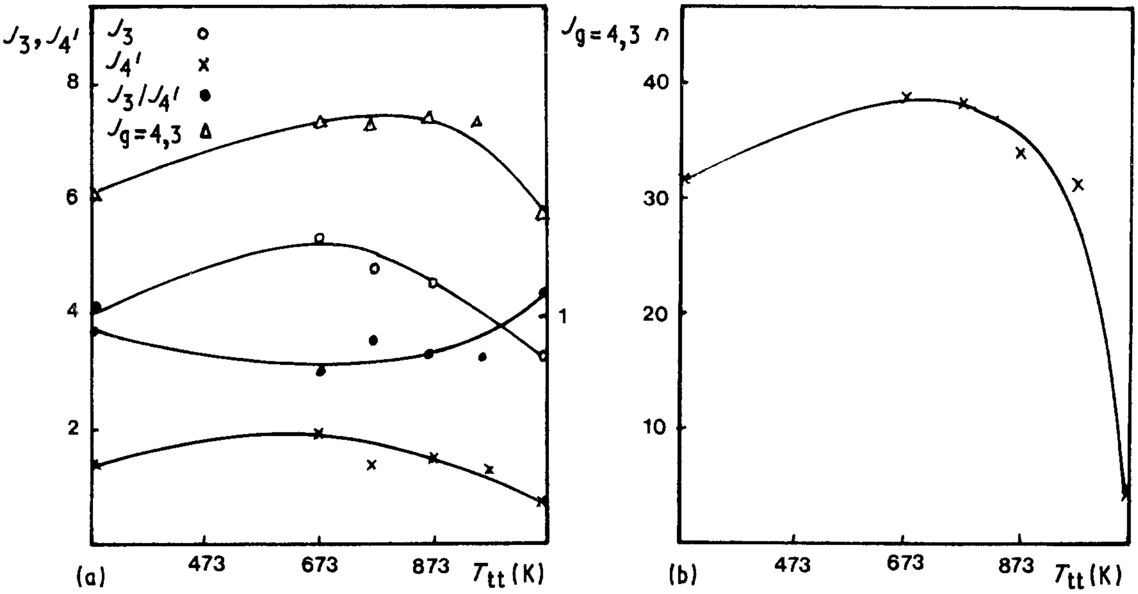

Figure 12 (a) The response signal amplitude, and (b) the non-linearity coefficient as functions of thermal treatment temperature (system 4).

of p-type. Because of this, the potential barrier on ZnO grain boundaries increased and broadened. At the same time, this concentration becomes maximal inside the pyrochlore phase. There is a same probability for the formation of γ-bismuth oxide phase in the intergranular layer with a higher ionic resistivity.

5. Conclusion

The results obtained indicate an obvious connection between the electrical characteristics of ZnO varistors and the concentration of impurity ions inside the zinc oxide grains. The best results were reached if there were no impurities inside the ZnO grains or on their surface layers (relating especially to bismuth but also to manganese ions). With an increase in calcination temperature, the degree of imperfection of the ZnO crystal lattice is reduced, as is the possibility of impurities diffusing into the surface layer. In such a way a more convenient shape of the potential barrier at the boundary of two grains was formed and a higher non-linearity was obtained. High cooling rates cause thermal stresses inside the samples, with a negative influence on non-linearity. Too low cooling rates also cause a decrease in the non-linearity coefficient because of a partial insertion of other impurities into ZnO lattice. An increase in sintering temperature and time results in an increase of non-linearity up to a critical value of impurity concentration. After that, it decreases because of evaporation of bismuth oxide.

Kalium oxide inhibits the diffusion of bismuth ions as well as of manganese ions to a great extent, causing a non-linear decrease. In the case of systems which were prereacted, the manganese concentration hardly changed with sintering temperature. The non-linearity decreases at temperatures of pyrochlore decomposition, when the excess quantity of bismuth in the system causes shrinkage of the potential barrier by diffusion into the surface layer of grains. A further fall in non-linearity is a consequence of bismuth evaporation. By subsequent thermal treatment the maximum improvement of non-linearity at 673 K was reached. This coincides with the minimum deformation of the area surrounding Mn^{2+} ions inside the grains and with the maximum deformation inside the pyrochlore phase. Because of this the increase in non-linearity may be connected with the decrease of impurity ion concentration in the surface layer of ZnO grains followed by a recovery of outstanding thermal stresses. In the case of samples which were subsequently thermally treated at over 1073 K, a new signal with $g \approx 3$ was observed, but at present we have not tried to investigate its nature.

Acknowledgements

The research was supported financially by

"MINEL" and the Serbian Research Fund. The authors are grateful to "MINEL" for permission to publish the results.

References

1. P. KOSTIĆ, O. MILOŠEVIĆ, D. USKOKOVIĆ, "Fizika, hemija i technologiija silikatnih materijala", edited by M. M. Ristić (Insitute of Technical Sciences of the SASA, Beograd, 1984) p. 187.
2. K. EDA, "Grain Boundaries in Semiconductors" (North-Holland, New York, Amsterdam, Oxford, 1982) p. 343.
3. R. EINZINGER, "Grain Boundaries in Semiconductors" (North Holland, New York, Amsterdam, Oxford, 1982) p. 343.
4. G. M. ZHIDOMIROV, JA. S. LEBEDEV, S. M. DOBRYAKOV, N. YA. STEINSHNEIDER, A. K. CHIRKOV, V. A. GUBANOV, "Interpretaciya sloznih spektrov EPR", (Nauka, Moscow, 1975).
5. N. N. TIKHOMIROVA, S. N. DOBRYAKOV, I. V. BIKOLAEVA, *Phys. Status Solidi (a)* **10** (1972) 593.
6. S. A. ALTSHULER, B. M. KOZIREV, "Elektronii paramagnitnii rezonans soedinenii elementov promezhutochnih grup" (Nauka Moskva, 1972).
7. V. LOU, "Paramagnitnii rezonans v tverdih telah" (Izdvo inostranoi literaturi, Moscow, 1962).
8. A. M. STONEHAM, "Theory of Defects in Solids", (Clarendon Press, Oxford, 1975).
9. P. KOSTIĆ, O. MILŠEVIĆ, D. USKOKOVIĆ , XXVIII Jugoslovenska konferencija ETAN, Struga, June (1983) No. 5, p. 59.
10. O. MILOŠEVIĆ, P. KOSTIĆ, V. PETROVIĆ, D. USKOKOVIĆ, *J. Sci. Sintering* **15** (1983) 121.
11. O. MILOŠEVIĆ, P. KOSTIĆ, I. GRŽETIĆ, M. STOJANOVIĆ, V. PETROVIĆ, D. USKOKOVIĆ, Proceedings of the 6th Yugoslav-German Meeting on Materials Science, edited by H. Stambolier *et al.* (Skopje University, Skopje, 1984) p. 113.
12. J. WONG, *J. Appl. Phys.* **46** (1975) 1827.

Received 12 March
and accepted 31 May 1984